University of Kurdistan

Department of Electrical Engineering

Linear Control Systems

Projects

Instructor: Dr. Q. Shafiee **Teaching Assistant:** N. Mohammadi

10 small projects are provided in the following. Groups of two (or maximum three) are chosen to work on a project as a team. All the techniques and methods you learn in this course should be applied to the system step by step. This will give you a chance to deepen your knowledge and better understand the course. At the end of semester, each group may choose another system and try to implement the linear control techniques they learn during the course. For each project, the following steps should be carried out:

1. Obtain the differential equation governing the system and the state-space model of it.
2. Obtain the Block diagram and SFG representations of the system.
3. Calculate the eigenvalues of the state-space representation and also calculate poles and zeroes of the system's transfer function.
4. Discuss the stability of the system.
5. Obtain the step response of the closed-loop and open-loop system.
6. Determine the sensitivity of the open-loop and closed-loop system to parameter k and one of the feedforward transfer function poles, then compare them. (Hint: k is a gain in the feedforward path, representing the controller).
7. Sketch the root locus of $KG(s)$ for all $0 < K < \infty$, and then determine maximum allowable gain for stable system.
8. Plot the frequency response (Bode plot and Nyquist Diagram) of both closed-loop (compensated) and open-loop (uncompensated) system.
9. Use Nyquist criterion to determine the range of k which system remains stable. Compare it with the range obtained in step 7.
10. Determine the gain margin and phase margin of the both compensated and uncompensated systems. Discuss the stability of the system.
11. Design a lead-lag and a PID compensator for the system to stabilize nonstable systems and improve the performance with the following specifications:
12. $OS\% = 10\%$ with shortest rise time.
13. Also investigate the impact of the three PID coefficients on the performance of the system. Then, try to design the PID parameters using a systematic approach.
14. Calculate the error constants and steady-state error of the uncompensated (no PID) and compensated system. Determine the type of the system.
15. Add any other item you may feel would enhance your report.
16. Provide a detailed report on your project using a standard template.

Note: You can use MATLAB as a powerful tool to perform calculations and to sketch plots.

Project 1. A human's ability to perform physical tasks is limited not by intellect but by physical strength. If, in an appropriate environment, a machine's mechanical power is closely integrated with a human arm's mechanical strength under the control of the human intellect, the resulting system will be superior to a loosely integrated combination of a human and a fully automated robot.

Extenders are defined as a class of robot manipulators that extend the strength of the human arm while maintaining human control of the task. The defining characteristic of an extender is the transmission of both power and information signals. The extender is worn by the human; the physical contact between the extender and the human allows the direct transfer of mechanical power and information signals. Because of this unique interface, control of the extender trajectory can be accomplished without any type of joystick, keyboard, or master-slave system. The human provides a control system for the extender, while the extender actuators provide most of the strength necessary for the task. The human becomes a part of the extender and "feels" a scaled-down version of the load that the extender is carrying. The extender is distinguished from a conventional master-slave system; in that type of system, the human operator is either at a remote location or close to the slave manipulator, but is not in direct physical contact with the slave in the sense of transfer of power. An extender is shown in Figure 1(a). The block diagram of the system is shown in Figure 1(b). Consider the proportional plus integral controller

$$G_c(s) = K_p + \frac{K_I}{s}$$

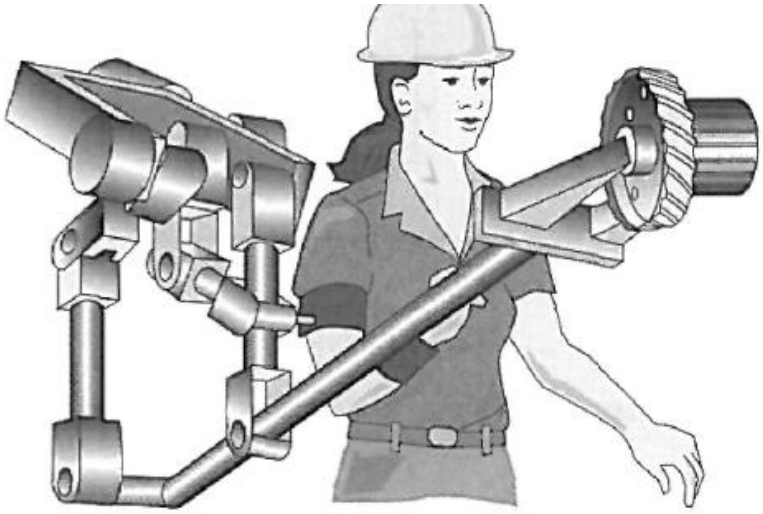

(a)

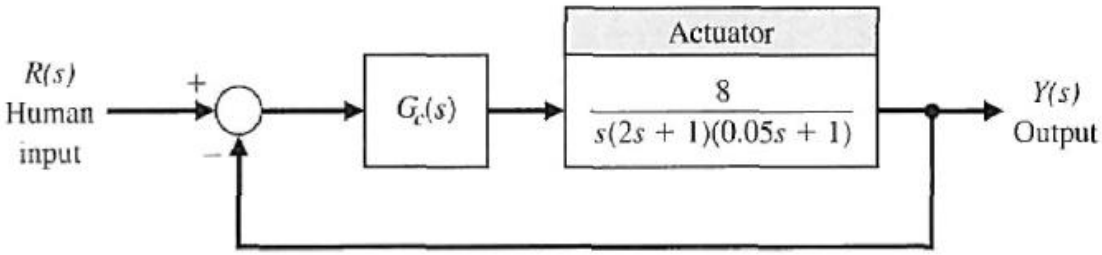

(b)

Figure 1

Project 2. A spacecraft with a camera is shown in Figure 2(a). The camera slews about 16° in a canted plane relative to the base. Reaction jets stabilize the base against the reaction torques from the slewing motors. Suppose that the rotational speed control for the camera slewing has a plant transfer function

$$G(s) = \frac{1}{(s+1)(s+2)(s+4)}$$

proportional controller is used in a system as shown in Figure 3(b), where

$$G_c(s) = K_p$$

and where $K_p > 0$.

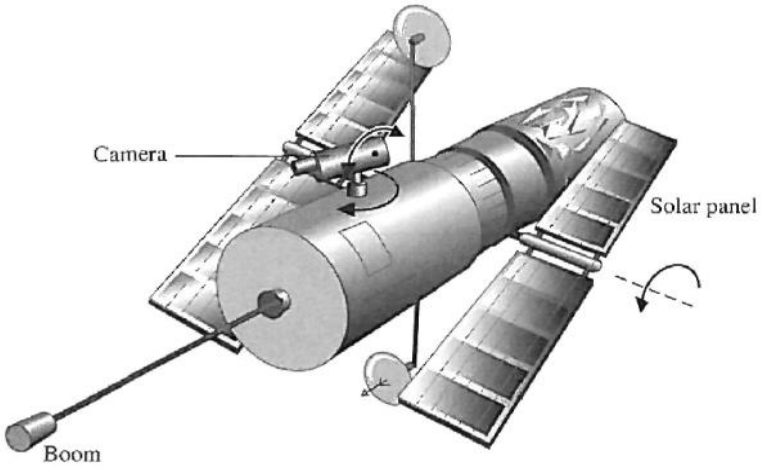

(a)

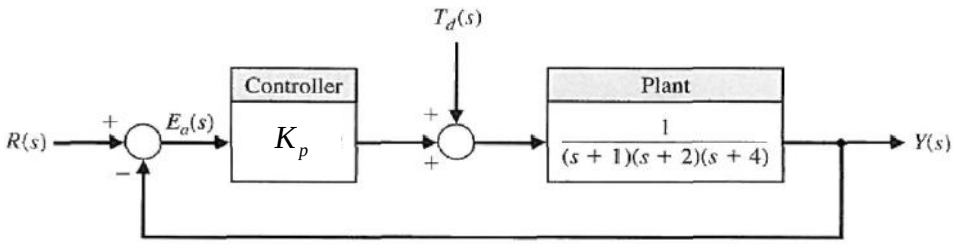

(b)

Figure 2

Project 3. The space satellite shown in Figure 3(a) uses control system to readjust its orientation, as shown in Figure 3(b).

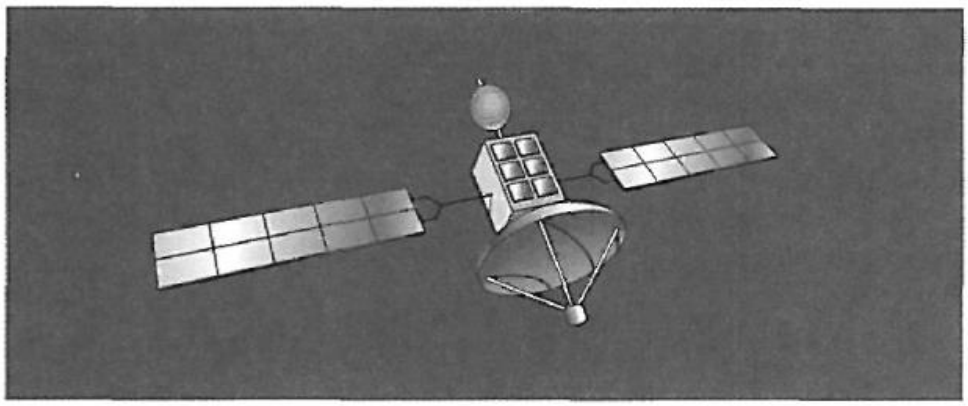

(a)

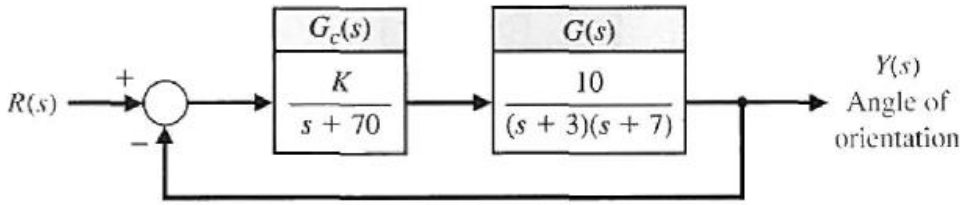

(b)

Figure 3

Project 4. A large antenna, as shown in Figure 4(a), is used to receive satellite signals and must accurately track the satellite as it moves across the sky. The control system uses an armature-controlled motor and a controller to be selected, as shown in Figure 4(b). The system specifications require a steady-state error for a ramp input r(r) = *Bi*, less than or equal to 0.01B, where *B* is a constant. We also seek a percent overshoot to a step input of *P.O.* < 5% with a settling time (with a 2% criterion) of *Ts* < 2 seconds.

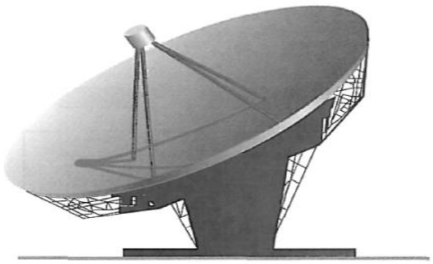

(a)

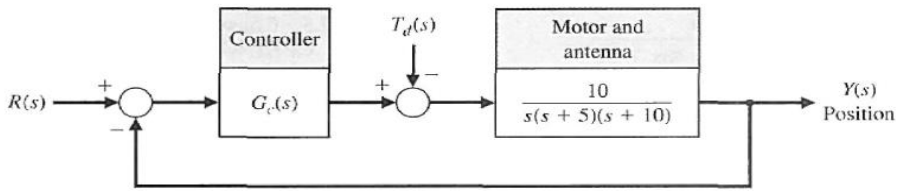

(b)

Figure 4

Project 5. The automatic control of an airplane is one example that requires multiple-variable feedback methods. In this system, the attitude of an aircraft is controlled by three sets of surfaces: elevators, a rudder, and ailerons, as shown in Figure 5(a). By manipulating these surfaces, a pilot can set the aircraft on a desired flight path.

An autopilot, which will be considered here, is an automatic control system that controls the roll angle φ by adjusting aileron surfaces. The deflection of the aileron surfaces by an angle θ generates a torque due to air pressure on these surfaces. This causes a rolling motion of the aircraft. The aileron surfaces are controlled by a hydraulic actuator with a transfer function $\frac{1}{s}$. The actual roll angle φ is measured and compared with the input. The difference between the desired roll angle $\varphi_d$and the actual angle φ will drive the hydraulic actuator, which in turn adjusts the deflection of the aileron surface. A simplified model where the rolling motion can be considered independent of other motions is assumed, and its block diagram is shown in Figure 5(b).

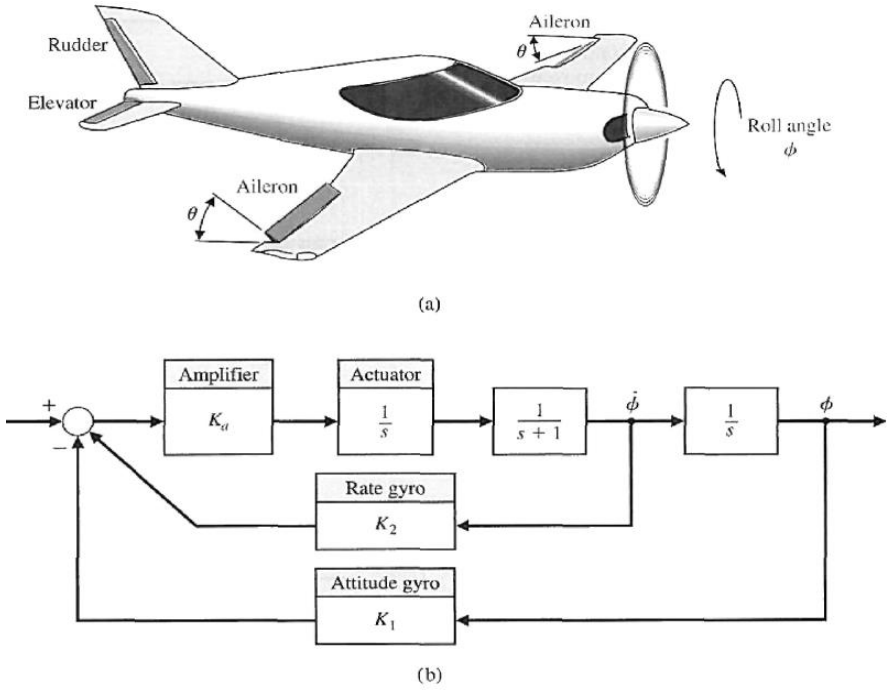

Figure 5

Project 6. A pilot crane control is shown in Figure 6(a). The trolley is moved by an input *F(t)* in order to control *x(t)* and *φ(t)*. The model of the pilot crane control is shown in Figure 6(b).

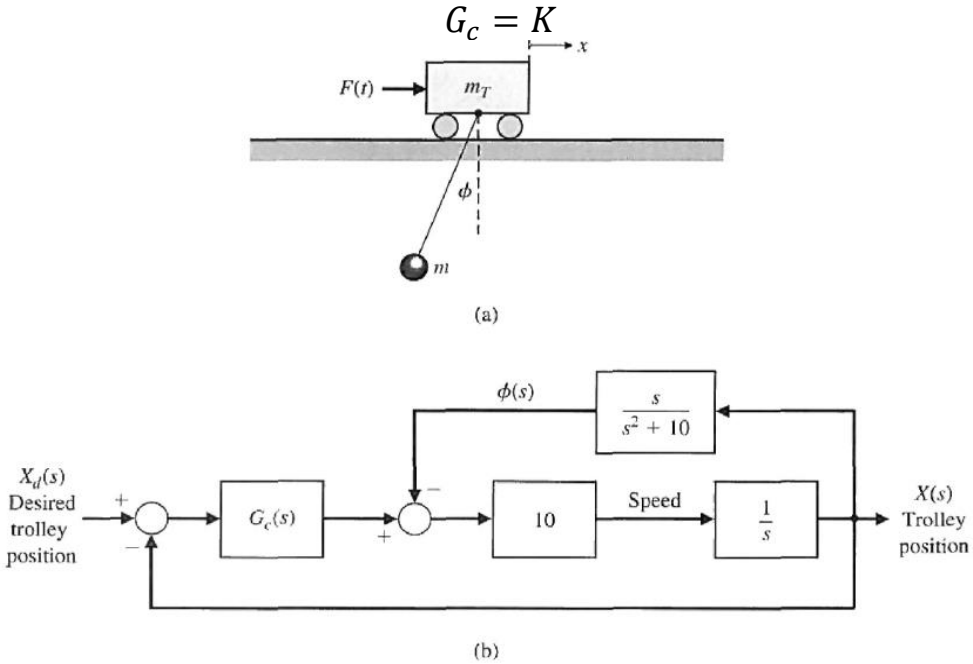

Figure 6

Project 7. A magnetically levitated high-speed train "flies" on an air gap above its rail system, as shown in Figure 7(a), The feedback control system is illustrated in Figure 7(b). The goal is to select K so that the response for a unit step input is reasonably damped and the settling time is less than 3 seconds. Sketch the root locus and select K so that all of the complex roots have a ζ greater than 0.6. Determine the actual response for the selected K and the percent overshoot.

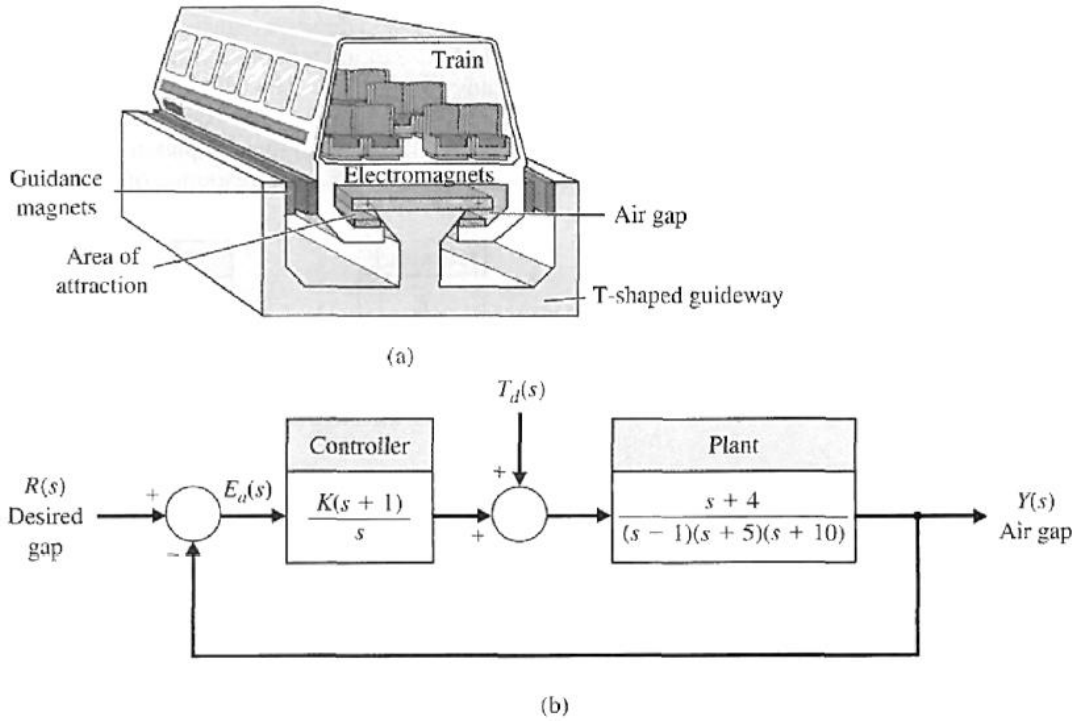

Figure 7

Project 8. A specialty machine shop is improving the efficiency of its surface-grinding process. The existing machine is mechanically sound, but manually operated. Automating the machine will free the operator for other tasks and thus increase overall throughput of the machine shop. The grinding machine is shown in Figure 8(a) with all three axes automated with motors and feedback systems. The control system for the y-axis is shown in Figure 8(b). To achieve a low steady-state error to a ramp command, we choose $K = 10$.

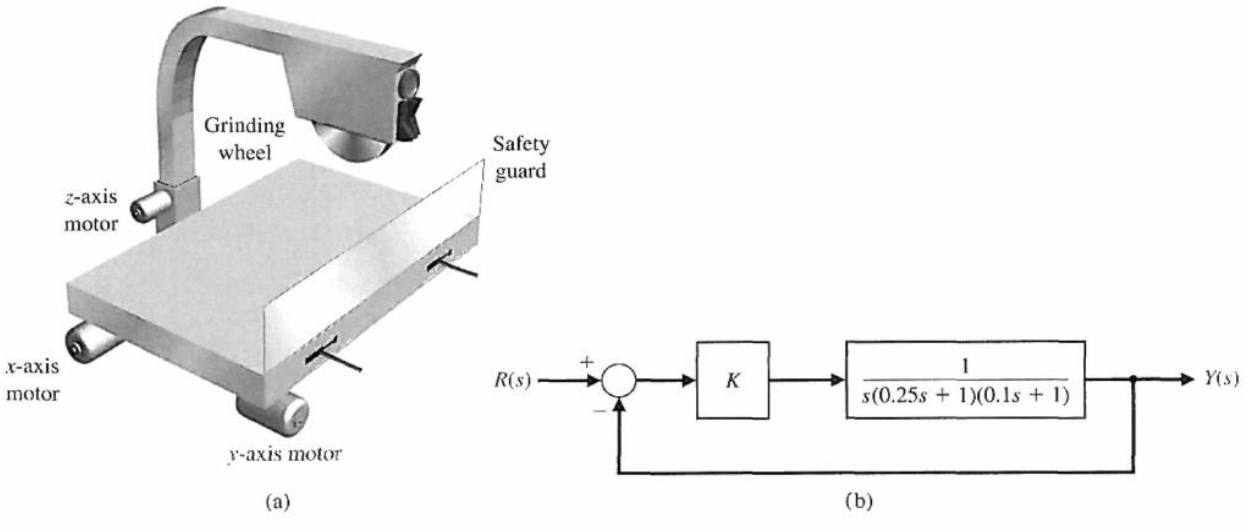

Figure 8

Project 9. In power systems, equilibrium is maintained between electromagnetic and mechanical torques of each connected synchronous generator. The change in electromagnetic torque of synchronous machine following a perturbation or disturbance can be resolved into a synchronizing torque component and a damping torque component. Nonoscillatory instability will be caused by insufficient synchronizing torque, whereas the lack of damping torque results in low frequency oscillations. Low frequency electromechanical oscillation (LFEO) is a phenomenon inherent to power systems. LEFO may endanger the dynamic stability of power systems if there is no proper control to damp these oscillations. Inter-area oscillations also limit the amount of power transfer on the tie-lines between the areas containing coherent generator groups. Therefore, it is very critical to design damping controllers to stabilize the oscillations. The block diagram of an interarea oscillation damping control is shown in Figure 9. Where the model of the interarea oscillation and sensor transfer function are

$$G(s) = \frac{1}{s^2 + 0.274s + 13.86}$$

$$H(s) = 1$$

Output of this control system is the phase difference between two areas and the control input (u) is damping torque which is generated by controller. One of the controllers which is used to damp oscillations in power systems is called power system stabilizer (PSS) which is installed on the synchronous generators.

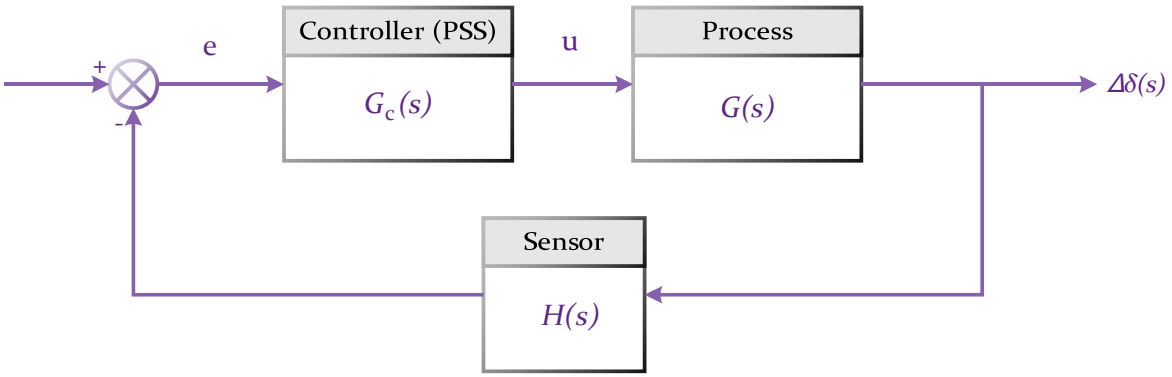

Figure 9

Project 10. In power systems, equilibrium is maintained between electromagnetic and mechanical torques of each connected synchronous generator. The change in electromagnetic torque of synchronous machine following a perturbation or disturbance can be resolved into a synchronizing torque component and a damping torque component. Nonoscillatory instability will be caused by insufficient synchronizing torque, whereas the lack of damping torque results in low frequency oscillations. Low frequency electromechanical oscillation (LFEO) is a phenomenon inherent to power systems. LEFO may endanger the dynamic stability of power systems if there is no proper control to damp these oscillations. Inter-area oscillations also limit the amount of power transfer on the tie-lines between the areas containing coherent generator groups. Therefore, it is very critical to design damping controllers to stabilize the oscillations. In this case study the impact of modulating the reactive power of a doubly-fed induction generator (DFIG) is studied. The flexible reactive power modulation ability of DFIG to damp power oscillations can be considered as another controller for damping purposes.

The nonlinear dynamic behavior of DFIG reactive power control loop is described as

$$\dot{\delta}_{12} = \omega_{12}$$

$$\dot{\omega}_{12} = -(\frac{1}{H_1} + \frac{1}{H_2})(\frac{V_1 V_2}{X})(\frac{\sin\delta_{12}}{\delta_{12}})$$

$$-(\frac{1}{H_1} + \frac{1}{H_2})\frac{\sin\delta_{12}}{\cos\delta_{12}}(\frac{V_2^2}{X} - \Delta Q_w - Q_w - Q_{s0})$$

$$\Delta\dot{Q}_w = \frac{u - \Delta Q_w}{T}$$

Where δ_{12} and ω_{12} are the relative rotor angle and relative rotor speed between two areas and also ΔQ_w is the controlled output reactive power of wind farm. Q_w is the rated output reactive power. u is the additional reactive power part (control signal).

The two-area power system as shown in Figure 10 is considered firstly. The two areas are connected through a 350km double ac transmission line with X=0.11 pu. The transmitted power between the two areas is 260MW at steady state. A DFIG-based wind farm represented by one aggregated DFIG is connected to the grid in Area I. The wind farm is equivalent by a DFIG with coordinated rate. The values of constant parameters are summarized in Table 1.

Table 1 Values of constant parameters

H_1	H_2	V_1	V_2	Q_w	Q_{s0}	T
13 s	12.5 s	0.9916 pu	1.003 s	0.15 pu	0.1	0.2 s

The control goal is to find u in such a way that the maximum overshoot of the relative speed response would be less than 10%.

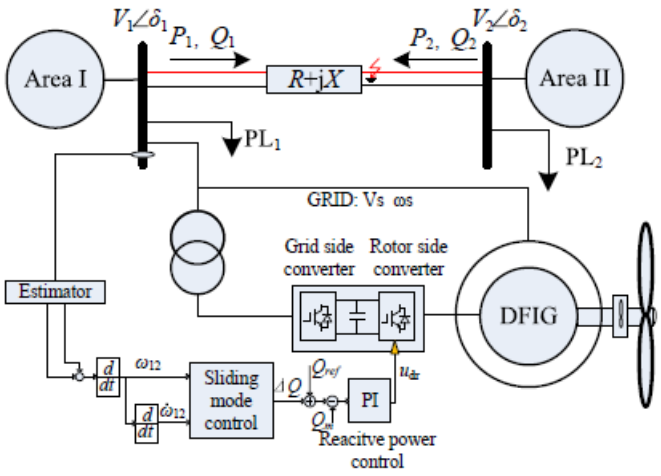

Figure 10: Two-area system with DFIG

Project 11. DC Motor

The mechanical-electrical model of the servo motor is presented in Figure 11.

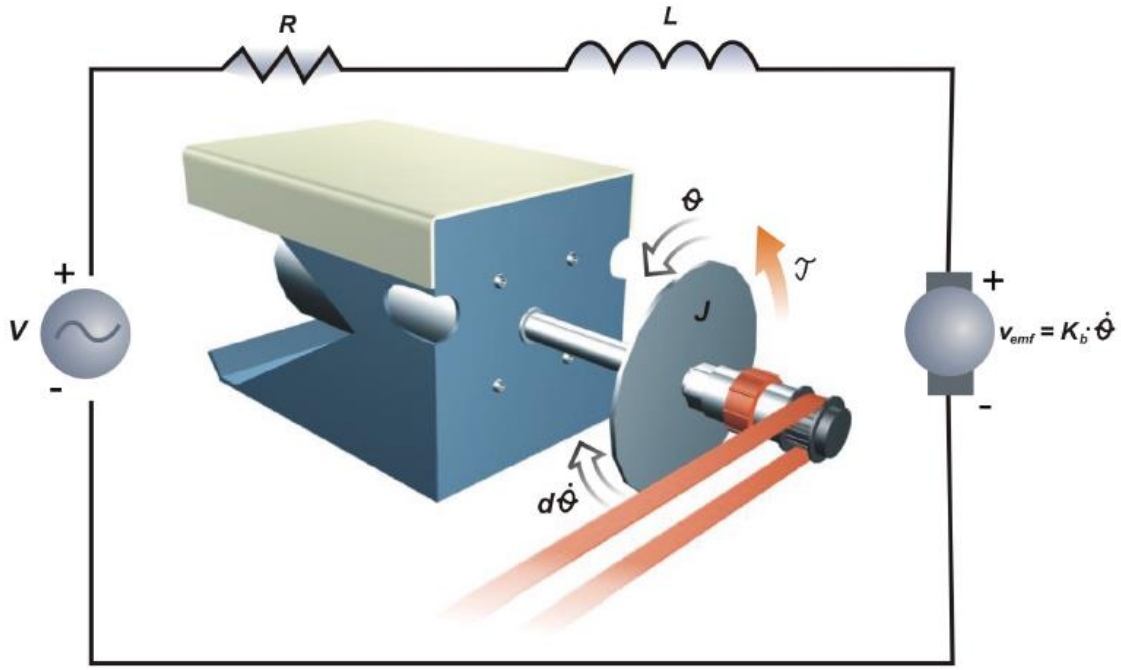

Figure 11: DC motor phenomenological model

Usually, phenomenological models are nonlinear, that means at least one of the states (i – current, θ– motor position) is an argument of a nonlinear function. In order to present such a model as a transfer function (a form of linear plant dynamics representation used in control engineering), it has to be linearized. However, for the DC motor model, nonlinearities are so small that they can be neglected.

The mathematical equations governing the DC motor system is as follows:

$$\frac{d}{dt}\begin{bmatrix}\omega \\ i\end{bmatrix} = \begin{bmatrix}-\frac{d}{J} & \frac{K_t}{J} \\ -\frac{K_b}{L} & -\frac{R}{L}\end{bmatrix} \cdot \begin{bmatrix}\omega \\ i\end{bmatrix} + \begin{bmatrix}0 \\ \frac{1}{L}\end{bmatrix} u$$

$$y = \begin{bmatrix}1 & 0\end{bmatrix}\begin{bmatrix}\omega \\ i\end{bmatrix}$$

Where $\omega = \frac{d\theta}{dt}$ is the angular velocity of the motor and other parameters are summarized in Table 2.

Table 2: values of the motor parameters

Parameter	Value
J- *moment of inertia*	$140 \cdot 10^{-7}\ kg \cdot m^2$
$\mathbf{K_t}$ - *torque constant*	*0.052 Nm/A*
$\mathbf{K_b}$- *electromotive force constant*	*0.057 Vs/rad*
d- *linear approximation of viscous friction*	$1 \cdot 10^{-6}$ *Nms/rad*
R- *resistance*	*2.5 Ω*
L - *inductance*	*2.5 mH*

Project 12. Magnetic Levitation model

The description of the Maglev setup in this section refers to the mechanical-electrical part and the control aspect. As shown in Figure 12, the Maglev unit consists of a Connection-Interface Panel with a Mechanical Unit on which a coil is mounted. An infra-red sensor is attached to the Mechanical Unit. Two steel spheres are included in the package.

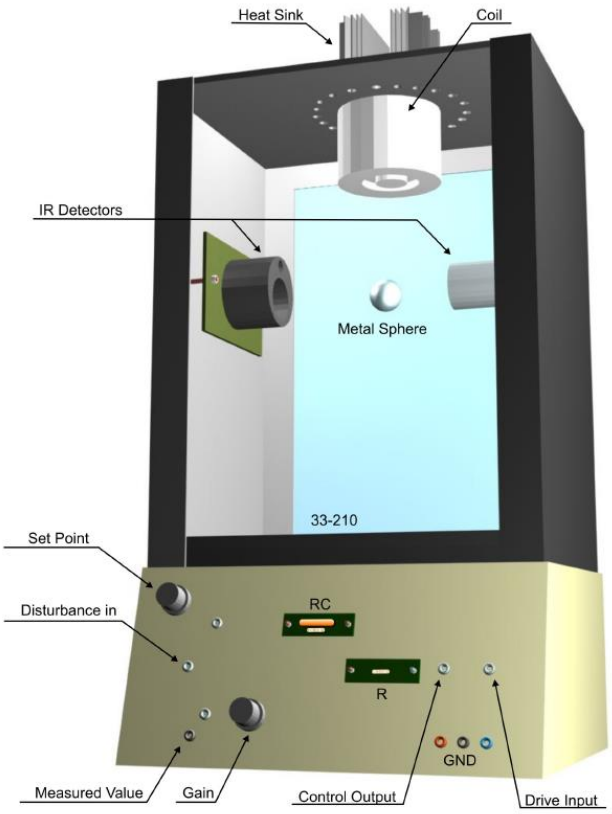

Figure 12: Maglev mechanical unit

Apart from the mechanical units, electrical units play an important role in Maglev control. They allow measured signals to be transferred to the PC via an I/O card. The Analogue Control Interface is used to transfer control signals from the PC to Maglev and back.

Every control project starts with plant modelling, so as much information as possible is given about the process itself. The mechanical-electrical model of Maglev is presented in Figure 13.

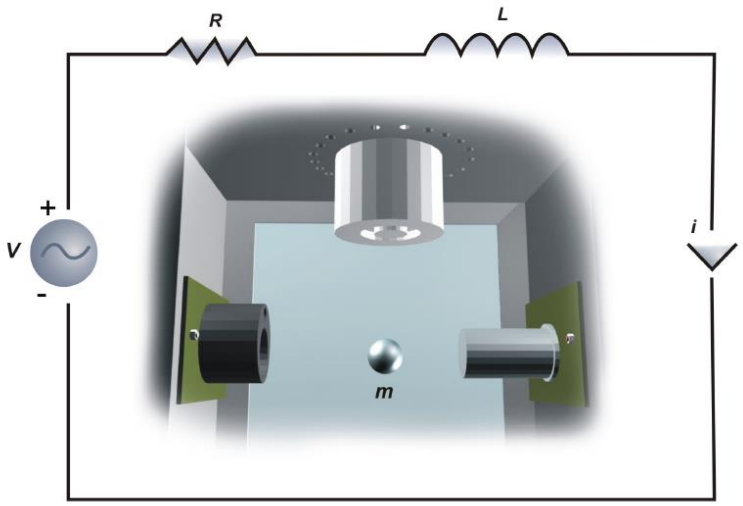

Figure 13: Maglev phenomenological model

According to the electrical-mechanical diagram presented in Figure 13 the nonlinear model equations can be derived. The simplest nonlinear model of the magnetic levitation system relating the ball position and the coil current *i* is the following:

$$m.\ddot{x} = m.g - k\frac{i^2}{x^2}$$

where *k* is a constant depending on the coil (electromagnet) parameters. To present the full phenomenological model a relation between the control voltage *u* and the coil current would have to be introduced analyzing the whole Maglev circuitry. However, Maglev is equipped with an inner control loop providing a current proportional to the control voltage that is generated for control purpose:

$$i = k_1 u$$

Equations (1) and (2) constitute a nonlinear model. The bound for the control signal is set to [-5V, +5V]. Maglev is a SISO plant – single input single output (Figure 14). Position is the model output and voltage is the control signal.

Figure 14: Maglev model for position control

Project 13. Pendulum

As shown in Figure 15 the pendulum setup consists of a cart moving along the 1-meter length track. The cart has a shaft to which two pendulums are attached and are able to rotate freely. The cart can move back and forth causing the pendulums to swing.

The movement of the cart is caused by pulling the belt in two directions by the DC motor attached at the end of the rail. By applying a voltage to the motor, we control the force with which the cart is pulled. The value of the force depends on the value of the control voltage. The voltage is our control signal. The two variables that are read from the pendulum (using optical encoders) are the pendulum position (angle) and the cart position on the rail. The controller's task will be to change the DC motor voltage depending on these two variables, in such a way that the desired control task is fulfilled (stabilizing in an upright position, swinging or crane control).

In order to design any control algorithms, one must understand the physical background behind the process and carry out identification experiments. The next section explains the modelling process of the pendulum.

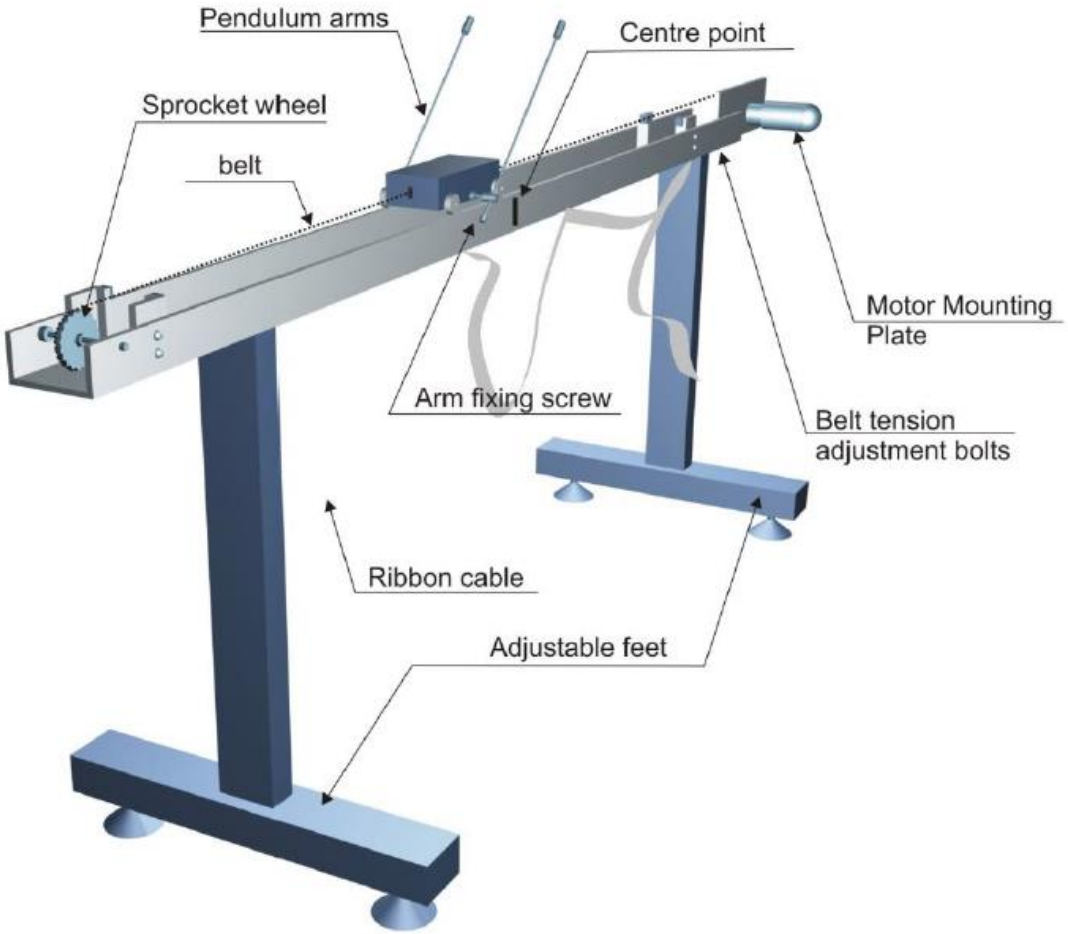

Figure 15: Digital Pendulum mechanical unit

Every control project starts with plant modelling, so as much information as possible is given about the process itself. The mechanical model of the pendulum is presented in Figure 14.

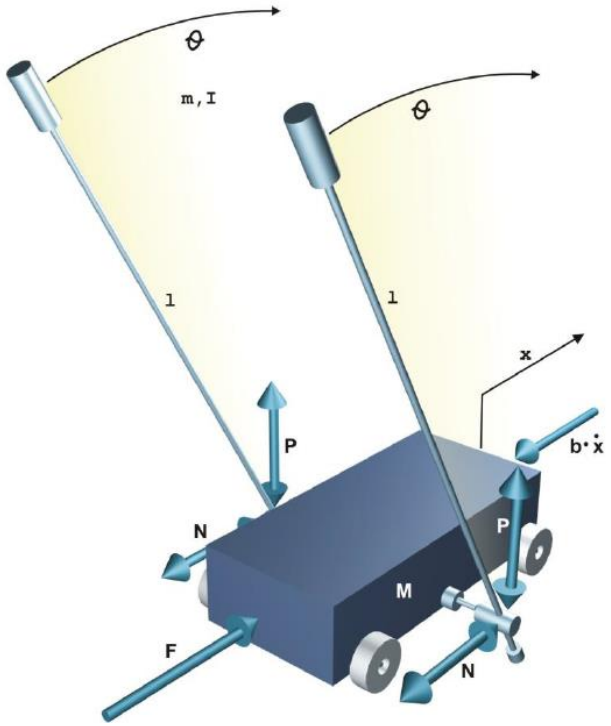

Figure 16: Pendulum phenomenological model

Summing the forces acting on the pendulum and cart system and the moments we obtain the following nonlinear equations of motion:

$$(m+M)\ddot{x}+b\dot{x}+ml\ddot{\theta}\cos\theta-ml\dot{\theta}^2\sin\theta=F$$
$$(I+ml^2)\ddot{\theta}-mgl\sin\theta+ml\ddot{x}\cos\theta+d\dot{\theta}=0$$

the values of all parameters are summarized in Table 3.

Table 3: Pendulum parameters

Parameter	Value
g- *gravity*	*9.81 m/s²*
l- *pole length*	*0.36 to 0.4 m - depending on the configuration*
M- *cart mass*	*2.4 kg*
m- *pole mass*	*0.23 kg*
I- *moment of interia of the pole*	*about 0.099 kg·m² - depends on the configuration*
b - *cart friction coefficient*	*0.05 Ns/m*
d - *pendulum damping coefficient*	*although negligible,necessary in the model- 0.005 Nms/rad*

Two things have to be kept in mind when designing the controllers. Both the cart position and the control signal are bounded in a real time application. The bound for the control signal is set to [–2.5V, +2.5V] and the generated force magnitude of around [–20.0N, +20.0N]. The cart position is physically bounded by the rail length and is equal to [-0.5m, +0.5m].

The pendulum is a SIMO plant – single input multiple output (Figure 17). The model described by above equations is still missing the translation between the force *F* and the actual control signal, which is the control voltage *u* that we supply with the PC control card. Assuming that the relation between the control voltage *u* and the generated cart velocity is linear, we might add the velocity vector generated by the motor to the model and ignore the *F* vector, or translate the control voltage *u* to the generated force *F* under the assumption that constant voltage will cause the cart to move with constant velocity:

$$F = k_{Fu}.\frac{du}{dt}$$

where k_{Fu} is the gain between the *u* voltage derivative and the *F* force.

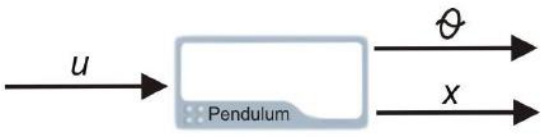

Figure 17: Pendulum model

Good Luck!